ELSEVIER

Pattern Recognition Letters 22 (2001) 631–637

Pattern Recognition Letters

www.elsevier.nl/locate/patrec

On calculation of fractal dimension of images

Ajay Kumar Bisoi [a,1], Jibitesh Mishra [b,*]

[a] *Department of Computer Science and Application, IGIT, Sarang 759 146, India*

[b] *Department of Computer Science and Application, College of Engineering and Technology, OUAT, Bhubaneswar 751 002, India*

Received 14 July 1999; received in revised form 27 June 2000

Abstract

Fractal geometry has gradually established its importance in the study of image characteristics. There are many techniques to estimate the dimensions of fractal surfaces. A famous technique to calculate fractal dimension is the grid dimension method popularly known as box-counting method. In this paper, we have found out a lower bound of the box size and provided the reason for having it. The study indicates the need for limiting the box sizes within certain bounds. © 2001 Elsevier Science B.V. All rights reserved.

Keywords: Box-counting; Fractal dimension; IFS generated fractal images

1. Introduction

Fractal geometry popularized by Mandelbrot (1982) has gained much support in the field of image analysis. Pentland (1984, 1986) provided the first theory in this respect by stating that fractal dimension correlates quite well with human perception of smoothness versus roughness of surfaces, with fractal dimension of 2 corresponding to smooth surfaces and fractal dimension of 3 corresponding to a maximum rough "salt-and-pepper" surface. Of course, he assumed the surface to be modeled by fractional Brownian function. However, it was followed by many other theories applicable to a wider class of fractals. Gangepain and Roques-Carmes (1986) described the popular reticular cell counting method and Keller et al. (1987, 1989) and Chen et al. (1990, 1993) gave even more interesting theories. Many studies are made to find the upper and lower bounds of the box size and in this regard (Chen et al., 1993) have given a theoretical justification for a restriction on the smallest box size inspired by the work of Pickover and Khorasani (1986). As we studied the cell counting method, we also found out the necessity of having a lower bound of the box size.

This paper is organized as follows. Section 2 describes various methods for calculating the fractal dimension. Section 3 discusses the reason for having upper and lower bounds of the box size. Section 4 gives a formula for finding the lower bound of the box size. Section 5 shows the experimental results. Concluding remarks are made in Section 6.

* Corresponding author. Tel.: (PBX) +91-674-402970/2868/2719/2669 Ext. 87; Tel.: (Dean) +91-674-407930; fax: +91-674-401043.

E-mail address: jibitesh@hotmail.com (J. Mishra).

[1] Tel.: +91-6760-40521; fax: +91-06760-40544.

PII: S0167-8655(00)00132-X

2. Methods for calculating fractal dimension

From the properties of self-similarity, fractal dimension D of a set A is defined as

$$D = \log(N)/\log(1/r), \tag{1}$$

where N is the total number of distinct copies similar to A and A is scaled down by a ratio of $1/r$.

Eq. (1) can be directly applied to geometrical fractals such as Sierpinski's Gasket or Cantor Dust and a theoretical estimation of fractal dimension is possible in such cases. However, for image surfaces, the value of N has to be computed using methods like box-counting and the fractal dimension is estimated phenomenologically.

2.1. Reticular cell counting method

In order to extend Eq. (1) to the world of images, Gangepain and Roques-Carmes (1986) introduced the cell counting method. If $M \times M$ is the size of an image and we imagine grids of size $L \times L$, then we can cover up the entire image by boxes of sides $L \times L \times L'$ in the vertical direction. Here $L' = \lfloor L \times G/M \rfloor$ can be a multiple of the gray level units where G represents the total number of gray levels. N is calculated by counting the total number of boxes that contain at least one gray level intensity surface. D is calculated by considering various L values, which in turn means various $1/r$ values as $1/r = M/L$, M being constant. From Eq. (1), we have

$$N \propto L^{-\mathrm{D}}, \text{ i.e. } N(L) \propto L^{-\mathrm{D}}. \tag{2}$$

For each L, the value of N is calculated and a log–log plot of N versus L is made. The slope of the least square linear fit line will be $-D$.

2.2. Keller's approach

Voss (1985) showed that the graph of an FBM also satisfies this power law. Eq. (2) holds for self-similar fractals as described by Roques et al. So Chen et al. (1993) proposed a modification of Eq. (2). Let $P(m,L)$ denote the probability that there are m intensity points within a box of size L centered about an arbitrary point of image intensity surface. Then

$$\sum_{m=1}^{N} P(m,L) = 1 \quad \forall L, \tag{3}$$

where N is the number of possible points in the box of side length L. If the image size is $M \times M$, then the total points on the image will be M^2. Thus, the expected number of boxes with side length L needed to cover the whole image is given by

$$N(L) = \sum_{m=1}^{N} \left(\frac{M^2}{m}\right) P(m,L) = M^2 \sum_{m=1}^{N} \frac{1}{m} P(m,L).$$

As

$$N(L) \propto L^{-\mathrm{D}}$$

hence

$$\sum_{m=1}^{N} \frac{1}{m} P(m,L) \propto L^{-\mathrm{D}}.$$

Let

$$N'(L) = \sum_{m=1}^{N} \frac{1}{m} P(m,L),$$

hence

$$N'(L) \propto L^{-\mathrm{D}}. \tag{4}$$

The fractal dimension D can be calculated by finding the slope of a log–log curve for a series of values of $N'(L)$ and L. To evaluate $P(m,L)$, a box of side L is moved around each point within the box. For every point find out the m value. Find out the frequency of occurrence of each m and divide it by the total number of points N within the box. This gives the $P(m,L)$ value of that particular m.

2.3. Differential box-counting method

Sarkar and Chaudhuri (1994) gave another method to find out the fractal dimension of images known as differential box-counting (DBC) method. Instead of counting the boxes like the cell counting method, they found out the minimum and maximum gray levels of the image in the (i,j)th grid, which may fall in the k and l box, respectively. Then

$$n_r(i,j) = l - k + 1 \tag{5}$$

is the contribution of the N_r in the (i,j)th grid. Taking contributions from all the grids,

$$N_r = \sum_{i,j} n_r(i,j).$$

N_r is counted for different values of r (i.e. in turn different values of L). Then using Eq. (1), D can be estimated from the least square linear fit of $\log(N_r)$ against $\log(1/r)$.

3. Bound of the box size

As we know box-counting is a very simple process. However, many researches have been performed to improve the procedures with respect to the calculation of the roughness accurately. Sometimes problems occur while estimating the roughness effectively due to improper limits and box size (Pickover and Khorasani, 1986; Chen et al., 1993; Feng et al., 1996). Of course, authors have taken various corrective measures. Many authors have assumed certain bounds according to the procedure adopted by them. Sarkar and Chaudhuri (1994) and Chaudhuri and Sarkar (1995) took a bound as $2 \leqslant L \leqslant M/2$ in his differential box-counting method.

3.1. Keller's correction

Keller and co-workers worked on the same aspect and also established a theoretical justification for the lower limit for the box size (Chen et al., 1993). They established it by stating that as the box size decreases, the number of boxes needed to cover the fractal set will increase according to the power law. However the maximum number of nonempty boxes will be equal to the total number of discrete points. Thus if L_B is the lower bound of the box size, then by power law:

$$L_B \propto (1/M)^{1/D}, \tag{6}$$

where M is the total number of points on the image and D is the fractal dimension. Further from the self-similarity property of fractals, if the entire image is contained within one box of size L_{max}, then the image S scaled down by a ratio r will have the property

$$Mr^D = 1, \text{ i.e. } M = (1/r)^D \text{ for box of size } L.$$

Also $L = rL_{max}$.

Hence $N(L) = (1/r)^D = (L_{max}/L)^D$ is the generalized formula.

By arithmetic manipulation, we have

$$L^D = \frac{(L_{max})^D}{N(L)}, \text{ i.e. } L = \left[\frac{(L_{max})^D}{N(L)}\right]^{1/D} = \frac{L_{max}}{[N(L)]^{1/D}}.$$

When the box size L goes on decreasing to a lower bound L_B, $N(L)$ will be equal M, then

$$L_B = \frac{L_{max}}{(M)^{1/D}}. \tag{7}$$

Keller et al. also proposed a procedure to first find out D with different L values and then follow an iterative procedure to produce L_B value using Eq. (7) and re-estimate the D for only box sizes of $L > L_B$. This iteration should continue till D is found out based on the box size of L_B. Of course he stated that the process will converge for ideal fractals only.

3.2. Fractional box-counting method

Feng et al. (1996) argued over the counting process. They pointed out that undercounting occurs in small scales and overcounting occurs in large scales in case there are uniform intensity areas. Because the intensity variance is zero for such areas and hence their contribution towards the fractal dimension is zero, they do but have a certain value. Hence in case of small scales, such areas are ignored and this results in undercounting. They particularly emphasized on this. Similarly in case of large scales we may take into account uniform intensity areas also giving rise to an overcounting. Therefore in order to avoid such problems, they proposed a fractional box-counting method where the shape of the boxes can be deformed, depending on the intensity levels.

Let $A \in S(X^m)$. If $\rho(n) = 2^{-n}$ is the counting scale, define $\rho_0 = 2^{-n-q}$ as the base scale for $n = 1, 2, 3, \ldots$ and $q = 1, 2, 3, \ldots$. Cover the space X^m by closed adjacent square boxes of side $\rho(n)$. Break each box at counting scale $\rho(n)$ further into boxes at base scale ρ_0. Let $\eta_n(A)$ and $\eta_0(A)$ denote

the number of boxes of size $\rho(n)$ and ρ_0 which intersect the set X^m, respectively. If A has box-counting dimension D then

$$D' = \lim_{n\to\infty}\{\ln(\eta_0(A))/\ln(1/\rho_0)\} = D \tag{8}$$

exists, and D' is called the fractional box dimension of A.

4. Proposed lower bound of the box size

According to Gangepain and Roques-Carmes (1986) $L' = \lfloor L \times G/M \rfloor$ and hence M/L number of vertical boxes on any grid as indicated in Fig. 1 will have a length of L', which can be a multiple of gray level units in the space. As the image intensity surface is quantized over the space, L' determines how many boxes contain at least one gray level intensity surface. Studying the cell counting method, we discussed that the imposition of a lower bound on the box size is necessary in order to calculate the roughness of a image surface accurately. The same constraint of the lower bound is applicable to all the other methodologies discussed in the preceding sections.

Let us consider the fundamental aspect of roughness, which implies a fractal dimension of 3 for the roughest possible surface. It can be noted that there are $L \times L = L^2$ pixels on a particular grid

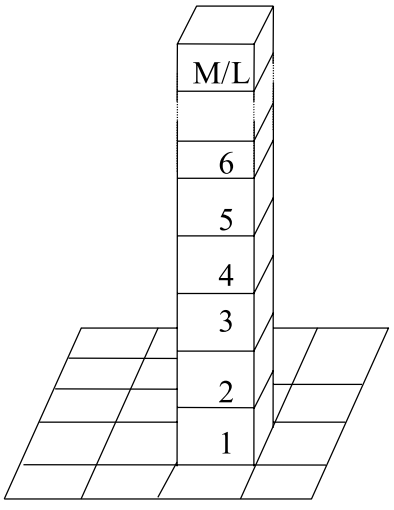

Fig. 1. The boxes on a particular grid in the vertical direction.

to correspond to all M/L number of vertical boxes on that grid. In order to obtain maximum roughness all the boxes on top of each grid should be countable, in which this case the total countable boxes are:

$$N_{\max} = \text{No. of grids } \times M/L$$
$$= M/L \times M/L \times M/L = [M/L]^3.$$

And applying Eq. (1) we will get dimension $D_{\max} = 3$ as $1/r = M/L$.

Similarly, the value of N is minimum when each grid contributes to only one box i.e. $N_{\min} = M/L \times M/L = [M/L]^2$, which implies $D_{\min} = 2$.

However, sometimes it may so happen that $L^2 < M/L$ and we cannot have all M/L boxes containing at least one gray level intensity surface. Hence in this case the possibility of getting maximum roughness has to be ruled out. Therefore, in order to obtain maximum roughness, we have to consider the box size such that

$$L^2 \geqslant M/L \Rightarrow L^3 \geqslant M. \tag{9}$$

Of course, roughness of the image is obtained by considering various L values and drawing a log–log plot of N versus L. But still the lower L values, which do not obey Eq. (9) will result in some incorrect points on the log–log plot and hence an incorrect D value. Therefore, the different L values should be taken such that Eq. (9) is satisfied.

Regarding the upper limit of the box size, we have to take a maximum box size up to $M/2$. Otherwise, even if we increase the L value more than $M/2$, we can have only one grid on the entire image covering a part of the image and hence we cannot count N. Thus, L should be chosen such that

$$L \leqslant M/2. \tag{10}$$

Therefore, we can choose the value of L such that it satisfies both Eqs. (9) and (10), which can provide us the accurate roughness of any image.

5. Experimental results

In order to find the fractal dimensions of images generated by us (Bisoi and Mishra, 1999) which

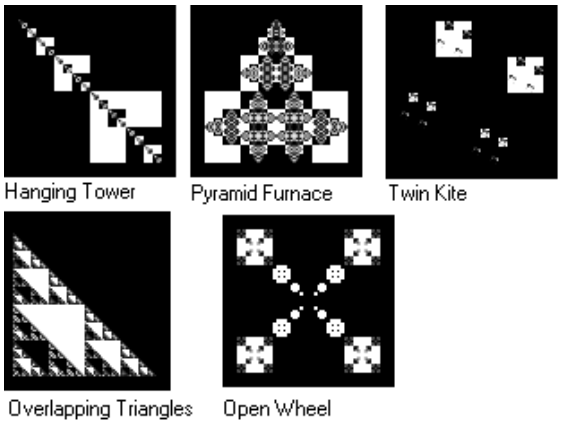

Fig. 2. Various images.

are shown in Fig. 2, we applied the various methods discussed in Section 2. The methods have been applied with and without the lower bound (as given by Eq. (9)) in order to estimate the fractal dimension; the upper bound is given by Eq. (10) being applicable in all cases. The images generated by us have used the IFS technique modified by incorporation of inverse replicas of images. The resulting estimates of fractal dimensions are shown in Table 1. It is evident that application of lower bound captures more roughness of the images. Chen et al. (1993) had already pointed out that "without having proper lower bounds, there is a bias in the curve fitting results, leading to the underestimation of the fractal dimension D". Our experiments also agree with it and it is observed that, if we are not using the lower bound of the box size we are in fact getting fractal dimensions less than the correct value. A calculation from this table shows that the fractal dimension may be underestimated by 1–3% in case of use of unrestricted box size.

We had calculated the fractal dimension as the slope of the best fit line of $\log(N)$ vs. $\log(1/r)$. The actual deviation of $\log(N_i)$ from the fitted straight line is given by $d_i = \log(N_i) - D \times \log(1/r_i)$. The square deviations d_i^2 are tabulated in Tables 2–4 up to 3 truncated digits after the decimal point for various methods applied with and without lower bound to some images. The parameter d_i^2 which is a measure of closeness of ith point to the line is given by:

$$d_i^2 = \{\log(N) - D \times \log(1/r)\}^2. \tag{11}$$

From the tables, the following observations are found:

1. It is found that the d_i^2 corresponding to small box sizes in all the methods are quite large as compared to other box sizes.
2. It is also found that the d_i^2 corresponding to the large box sizes are also large.

The first point agrees to our theoretical justification of lower bound of box size. It suggests that we should omit box of size 2, 3, 4 in an 80×80 image as $L^3 \geqslant M$. The second point has no known theoretical justification, which was also pointed out by Chen et al. (1993) in their experiments. They had discussed that the points coming from large box sizes also deviate from the ideal linear relationship. However, it is to be noted the computation of lower bound by Keller et al. is a probabilistic one and is applicable for ideal fractals only. Whereas our method is deterministic and is applicable for all images. Moreover our method is applicable to

Table 1
Fractal dimensions of images obtained by various methods

Images	Methods					
	Cell counting		Keller's method		Differential box-counting	
	Without lower bound	With lower bound	Without lower bound	With lower bound	Without lower bound	With lower bound
Overlapping triangles	2.167198	2.228188	2.441961	2.485951	2.583887	2.656982
Pyramid furnace	2.211895	2.290588	2.461466	2.508177	2.676281	2.77429
Open wheel	2.176739	2.248505	2.669181	2.742272	2.578142	2.669402
Twin kite	2.12107	2.181195	2.81634	2.909173	2.382044	2.475039
Hanging tower	2.108768	2.141283	2.487009	2.54193	2.343462	2.401505

Table 2
Square deviations in the cell counting method without and with lower bound

Box size	Overlapping triangles		Pyramid furnace		Open wheel		Twin kite		Hanging tower	
	Without lower bound	With lower bound	Without lower bound	With lower bound	Without lower bound	With lower bound	Without lower bound	With lower bound	Without lower bound	With lower bound
2	0.038	0.086	0.067	0.149	0.05	0.115	0.03	0.073	0.023	0.042
4	0.008	0.029	0.012	0.045	0.012	0.042	0.011	0.034	0	0.001
5	0.006	0.024	0.011	0.041	0.016	0.045	0.014	0.036	0.011	0.021
8	0	0.004	0	0.004	0	0.001	0	0.004	0	0
10	0	0.002	0	0.004	0	0.007	0	0.004	0.002	0.005
16	0.007	0.001	0.013	0.003	0.019	0.008	0.016	0.007	0.016	0.011
20	0.008	0.003	0.013	0.004	0.004	0	0	0	0	0
40	0.037	0.03	0.056	0.045	0.061	0.051	0.07	0.06	0.02	0.017

Table 3
Square deviations in the Keller's method without and with lower bound

Box size	Overlapping triangles		Pyramid furnace		Open wheel		Twin kite		Hanging tower	
	Without lower bound	With lower bound	Without lower bound	With lower bound	Without lower bound	With lower bound	Without lower bound	With lower bound	Without lower bound	With lower bound
3	0.243	0.309	0.275	0.349	0.673	0.855	1.086	1.379	0.38	0.482
5	0.133	0.175	0.134	0.179	0.329	0.438	0.583	0.766	0.21	0.275
7	0.075	0.102	0.075	0.105	0.165	0.234	0.372	0.502	0.12	0.164
9	0.04	0.059	0.042	0.063	0.123	0.176	0.191	0.276	0.07	0.1
11	0.022	0.035	0.021	0.034	0.076	0.115	0.075	0.125	0.036	0.056
13	0.01	0.018	0.009	0.018	0.037	0.063	0.028	0.058	0.016	0.029
15	0.003	0.008	0.003	0.008	0.014	0.029	0.015	0.036	0.006	0.013
17	0	0.002	0	0.002	0.002	0.01	0.002	0.012	0	0.004
19	0	0	0	0	0	0.001	0	0.001	0	0
21	0.002	0	0.002	0	0.003	0	0.005	0	0.003	0
23	0.005	0.002	0.006	0.003	0.013	0.005	0.016	0.006	0.01	0.005
25	0.011	0.007	0.011	0.007	0.027	0.016	0.035	0.019	0.019	0.012
27	0.018	0.013	0.018	0.012	0.046	0.032	0.061	0.041	0.029	0.021
29	0.025	0.02	0.026	0.019	0.069	0.053	0.096	0.072	0.041	0.032
31	0.033	0.027	0.034	0.027	0.095	0.078	0.14	0.113	0.053	0.043
33	0.042	0.035	0.043	0.036	0.125	0.106	0.192	0.162	0.067	0.056
35	0.051	0.044	0.052	0.045	0.156	0.136	0.251	0.219	0.081	0.07
37	0.061	0.054	0.062	0.054	0.189	0.168	0.318	0.284	0.096	0.085
39	0.071	0.064	0.072	0.065	0.223	0.202	0.392	0.356	0.11	0.099

all the fractal dimension estimation techniques as it can be seen from Tables 2–4. Bounds discussed by other researchers are only applicable to their own methods.

6. Concluding remarks

Due to growing importance of box-counting methods on calculation of fractal features from an image, we established a lower bound of the box size to ensure accurate results. Our study corroborates the following intuitive observations.

With too low a box size, the maximum number of boxes above a grid would be more than the number of available intensity levels. The resulting unaccounted boxes would lead to an underestimation of fractal dimension. On the other hand, for too high a box size, the number of boxes would be much less than the number of intensity levels. For example,

Table 4
Square deviations in the differential box-counting method without and with lower bound

Box size	Overlapping triangles		Pyramid furnace		Open wheel		Twin kite		Hanging tower	
	Without lower bound	With lower bound	Without lower bound	With lower bound	Without lower bound	With lower bound	Without lower bound	With lower bound	Without lower bound	With lower bound
2	0.134	0.234	0.233	0.41	0.184	0.331	0.15	0.288	0.094	0.16
4	0	0.005	0	0.011	0	0.014	0.002	0.029	0.001	0.001
5	0.003	0.001	0	0.007	0.004	0.03	0.029	0.081	0.023	0.049
8	0.001	0.001	0.005	0	0.019	0.002	0.014	0	0.021	0.008
10	0.004	0	0.006	0	0.001	0.002	0.008	0	0.001	0.008
16	0.001	0	0.005	0	0.02	0.006	0.039	0.017	0.042	0.027
20	0.006	0.001	0.01	0.002	0.002	0	0	0.001	0.001	0
40	0.004	0.002	0.009	0.004	0.016	0.009	0.034	0.024	0.005	0.003

for $L = M/2$, there will be just two boxes above a grid and a 50% variation in the intensity level and roughness of the fractal surface would go unnoticed. The behavior at the extreme L values leads us to speculate about the existence of an optimum value for L corresponding to the best estimate of fractal dimension. This ideal value for L would be around $L = M/G$ which will give rise to as many vertical boxes as there are intensity levels, thereby ensuring accounting of minute variation in intensity. It is hoped that this study will stimulate further research in the direction of obtaining appropriate box sizes, which will give more accurate results.

References

Bisoi, A.K., Mishra, J., 1999. Fractal images with inverse replicas. Machine Graphics and Vision 8 (1), 77–82.

Chaudhuri, B.B., Sarkar, N., 1995. Texture segmentation using fractal dimension. IEEE Trans. Pattern Anal. Machine Intell. 17 (1), 72–77.

Chen, S., Keller, J.M., Crownover, R., 1990. Shape from fractal geometry. Artificial Intell. 43, 199–218.

Chen, S.S., Keller, J.M., Crownover, R.M., 1993. On the calculation of fractal features from images. IEEE Trans. Pattern Anal. Machine Intell. 15 (10), 1087–1090.

Feng, J., Lin, W.-C., Chen, C.-T., 1996. Fractional box-counting approach to fractal dimension estimation. In: Proc. ICPR'96, 1996, pp. 854–858.

Gangepain, J., Roques-Carmes, C., 1986. Fractal approach to two dimensional and three dimensional surface roughness. Wear 109, 119–126.

Keller, J.M., Crownover, R.M., Chen, R.Y., 1987. Characteristics of natural scenes related to the fractal dimension. IEEE Trans. Pattern Anal. Machine Intell. 9 (5), 621–627.

Keller, J.M., Chen, S., Crownover, R.M., 1989. Texture description through fractal geometry. Comput. Vision Graphics Image Process. 45, 150–166.

Mandelbrot, B.B., 1982. The Fractal Geometry of Nature. W.H. Freeman, Sans Francisco.

Pentland, A.P., 1984. Fractal based description of natural scenes. IEEE Trans. Pattern Anal. Machine Intell. PAMI-6, 661–674.

Pentland, A.P., 1986. Shading into texture. Artificial Intell. 29, 147–170.

Pickover, C.A., Khorasani, A.L., 1986. Fractal characterization of speech waveform graphs. Comput. Graphics 1 (1), 51–61.

Sarkar, N., Chaudhuri, B.B., 1994. An efficient differential box-counting approach to compute fractal dimension of image. IEEE Trans. Systems, Man. Cybernet. 24 (1), 115–120.

Voss, R., 1985. Random fractals: characterization and the measurement. In: Pynn, R., Skjeltorp, A. (Eds.), Scaling Phenomena in Disordered Systems. Plenum, New York.